Inonotsuoxide B suppresses hepatic stellate cell activation and proliferation via the PI3K/AKT and ERK1/2 pathway

JUAN JIN[1,2*], HUI YANG[1*], LILI HU[1,3*], YINGHONG WANG[4], WENYONG WU[5], CHENGMU HU[1,3], KUN WU[1,3], ZEHUA WU[1,3], WENMING CHENG[1,6] and YAN HUANG[1,3]

[1]Inflammation and Immune Mediated Diseases Laboratory of Anhui Province; [2]School of Basic Medical Sciences; [3]Department of Pharmacology, School of Pharmacy, Anhui Medical University, Hefei, Anhui 230032; [4]Department of Pharmacy, Division of Life Sciences and Medicine, Anhui Provincial Cancer Hospital, The First Affiliated Hospital of University of Science and Technology of China, Hefei, Anhui 230001; [5]Department of General Surgery, Anhui No. 2 Provincial People's Hospital, Hefei, Anhui 230041; [6]Department of Natural Medicine and Chemistry, School of Pharmacy, Anhui Medical University, Hefei, Anhui 230032, P.R. China

Received September 4, 2019; Accepted August 4, 2020

DOI: 10.3892/etm.2022.11344

Abstract. Hepatic stellate cells (HSCs) serve a pivotal role in the formation and degradation of the extracellular matrix during liver fibrosis. Inonotsuoxide B is a tetracyclic triterpenoid that can be extracted from *Inonotus obliquus* and has been previously reported to inhibit the growth of liver and gastric cancer cells. However, its effect on liver fibrosis remain poorly understood. Therefore, in the present study, the potential antiproliferative effects of inonotsuoxide B on HSCs was investigated. Initially, cells were divided into the following five groups: Control; platelet-derived growth factor (PDGF)-BB (10 ng/ml); and PDGF-BB + inonotsuoxide B (5, 10 and 20 μg/ml) groups. Inonotsuoxide B treatment (5, 10 and 20 μg/ml) was revealed to reverse PDGF-BB-induced HSC proliferation. Furthermore, the protein expression of α-smooth-muscle actin (α-SMA) and type I collagen was significantly decreased in the inonotsuoxide B (10 and 20 μg/ml) groups compared with the PDGF-BB group. Inonotsuoxide B (5, 10 and 20 μg/ml) was also revealed to suppress PDGF-BB-induced α-SMA mRNA expression and activation of the PI3K/AKT and ERK signaling pathways in HSCs. These findings suggest that inonotsuoxide B suppresses the proliferation and activation of HSCs by inhibiting the PI3K/AKT and ERK1/2 signaling pathways.

Correspondence to: Professor Yan Huang, Department of Pharmacology, School of Pharmacy, Anhui Medical University, 81 Meishan Road, Hefei, Anhui 230032, P.R. China
E-mail: aydhy@126.com

Professor Wenming Cheng, Department of Natural Medicine and Chemistry, School of Pharmacy, Anhui Medical University, 81 Meishan Road, Hefei, Anhui 230032, P.R. China
E-mail: 914341547@qq.com

*Contributed equally

Abbreviations: HSCs, hepatic stellate cells; PDGF, platelet-derived growth factor; COL-I, type I collagen; α-SMA, α-smooth-muscle actin

Key words: liver fibrosis, hepatic stellate cells, *Inonotus obliquus*, inonotsuoxide B, platelet-derived growth factor

Introduction

Hepatic fibrosis (HF) is characterized by the abnormal secretion and degradation of the extracellular matrix (ECM) in the liver that may be caused by a number of different factors, including viral infection, alcohol consumption and drug abuse (1). HF is considered to be a healing reaction to liver injury, which if occurs in excess, can eventually develop into cirrhosis (2). The majority of pharmacological agents that are currently being investigated have been suggested to exert weak antifibrotic and also certain hepatoprotective effects (3). In particular, inhibition of hepatic stellate cell (HSC) proliferation is considered to be an important component for both preventing and subsequently treating HF, as in chronic liver injury HSCs are activated, proliferate and produce abundant ECM, thereby differentiating into myofibroblasts (4).

Ionotus obliquus, commonly known as Chaga, is a medicinal fungus (order, Hymenochaetales; division, Basidiomycota) that primarily grows on birch in the temperate regions or cold northern climates (5). *Ionotus obliquus* has been previously reported to exhibit anticancer, antiaging and hepatoprotective effects (6). In recent years, there has been an increasing number of studies exploring the clinical application of *Inonotus obliquus* and determining its biologically active ingredients (7). Inonotsuoxide B is considered to serve a role in mediating the effects of *Ionotus obliquus* and can be isolated by silica, octadecylsilane and Sephadex LH-20 column chromatography as white, needle-like crystals (8). The structure and composition of inonotsuoxide B have been previously confirmed by mass

spectrometry, ^{1}H- and ^{13}C-nuclear magnetic resonance spectral data, where inonotsuoxide B has been referenced previously in published literature as a tetracyclic triterpenoid (8). Although tetracyclic triterpenoids have been previously suggested to potentially inhibit the proliferation of hepatocytes and gastric cancer cells, the potential antifibrotic effects of this compound remain poorly understood. Therefore, the present study examined the *in vitro* effects of inonotsuoxide B isolated from *Inonotus obliquus* on platelet-derived growth factor (PDGF)-BB-induced HSC proliferation and activation.

Materials and methods

Cells and reagents. Inonotsuoxide B was provided by Dr. Wenming Cheng, Department of Natural Medicine and Chemistry, School of Pharmacy, Anhui Medical University (Hefei, China). The rat hepatic stellate cell line HSC-T6 was purchased from Jiangsu KeyGEN BioTECH Corp., Ltd. PDGF-BB was obtained from PeproTech China. TRIzol® reagent was purchased from Thermo Fisher Scientific, Inc. (cat. no. 14050) and TB Green™ Premix Ex Taq™ II kit was purchased from Takara Biotechnology Co., Ltd. (cat. no. AH80340A). The following antibodies were used: Anti-α-smooth-muscle actin (α-SMA; cat. no. bs-10196R; lot. no. AG0734630), anti-collagen I (COL-I; cat. no. bs-10423R; lot no. AE120941; both from BIOSS), anti-AKT (cat. no. ESAP12208; Elabscience, Inc.), anti-phosphorylated (p)-AKT (cat. no. AF0016; lot no. 17q2826; Affinity Biosciences), anti-PI3K (cat. no. bsm-33219M; lot no. AH01181961; BIOSS), anti-phosphorylated (p)-PI3K (cat. no. ab138364; lot no. GR154304-8; Abcam), anti-p-ERK (cat. no. WL2201; lot no. I09051512), anti-ERK (cat. no. WL02371; lot no. I04102371; both from Wanlei Biological Technology Co., Ltd.), anti-β-actin (cat. no. TA-09; lot no. 19C10511; OriGene Technologies, Inc.), horseradish peroxidase (HRP)-conjugated anti-rabbit (cat. no. S0001; lot no. 56j9958; Affinity Biosciences) and HRP-conjugated anti-mouse (cat. no. ZB-2305; lot no. 193701224, OriGene Technologies, Inc.).

Cell culture and drug preparation. The purchased frozen HSC-T6 cells were transferred to DMEM (Nanjing Wisent Biological Co., Ltd.) containing 5% FBS (Hangzhou Sijiqing Biological Engineering Materials Co., Ltd.) and cultured at 37˚C with 5% CO_2. The culture medium was replaced every 2 days and cells were sub-cultured every 2-3 days. Following three passages, cells in a logarithmic growth phase were used for subsequent experiments.

Solid inonotsuoxide B crystals were dissolved in DMSO at a concentration of $1x10^5$ μg/ml.

Cell treatment. HSC-T6 cells were collected and seeded into a 96-well culture plate at a concentration of $1x10^4$ cells/well or HSC-T6 cells were seeded at a concentration of $1x10^5$/ml into a six-well culture plate and incubated in DMEM containing 5% FBS and cultured at 37˚C with 5% CO_2 (9). The cells were then divided into the following five groups: Control, PDGF-BB (10 ng/ml) and PDGF-BB + inonotsuoxide B (5, 10 and 20 μg/ml). Following culture for 24 h at 37˚C, the medium was changed to serum-free DMEM and appropriate concentrations of inonotsuoxide B were added to the PDGF-BB + inonotsuoxide B groups. After 30 min, apart from the control group that did not receive any treatment, all other groups were treated with PDGF-BB.

The experimental groups used for treatment with the PI3K inhibitor LY294002 were as follows: Control, PDGF-BB (10 ng/ml), PDGF-BB + inonotsuoxide B (20 μg/ml) and PDGF-BB + LY294002 (20 nmol/l). HSC-T6 cells were seeded at a concentration of $1x10^5$/ml into a six-well culture plate and incubated at 37˚C with 5% CO_2. Following culture for 24 h at 37˚C, the medium was changed to serum-free DMEM and innotsuoxide B (20 μg/ml) and LY294002 (20 nmol/l) were added to PDGF-BB + inootsuoxide B group and PDGF-BB + LY294002 group, respectively. Following incubation at 37˚C for 30 min, all groups received PDGF-BB treatment except for the control group that did not receive any treatment. Following incubation for 24 h at 37˚C, the cells were lysed in RIPA lysis buffer. The experimental groups used for treatment with the ERK inhibitor UO126 were as follows: Control, PDGF-BB (10 ng/ml), PDGF-BB + inonotsuoxide B (20 μg/ml) and PDGF-BB + UO126 (20 nmol/l). The aforementioned experimental method was followed.

Cell cytotoxicity measurement. HSC-T6 cells were collected and seeded into a 96-well culture plate at a concentration of $1x10^4$ cells/well (8) and divided into seven groups: Control, inonotsuoxide B (5, 10, 20, 40 and 80 μg/ml) and DMSO (0.1 μl). A total of four duplicate wells were used for each group, with 100 μl cell suspension per well. The outer wells were filled with 100 μl PBS and the plate was incubated in an incubator at 37˚C with 5% CO_2 for 8 h. Following attachment of the cells, the medium was replaced with serum-free DMEM. DMSO was added to the DMSO groups, whilst solutions of inonotsuoxide B at the stated concentrations were added to the cells designated to the inonotsuoxide B groups. Following 24 h, the culture medium was discarded and 20 μl MTT solution (5 mg/ml) were added to each well. Following incubation at 37˚C for 4 h, the supernatant was discarded and 150 μl DMSO were added to each well and incubated on a shaker at 37˚C for 10 min. The absorbance of each well was measured at 570 nm (10).

Cell viability assay. Before the effect of inonotsuoxide B on cell viability in the presence of PDGF-BB was determined using the MTT assay, HSC-T6 cells were collected. The cells were then divided into the following five groups: Control, PDGF-BB (10 ng/ml) and PDGF-BB + inonotsuoxide B (5, 10 and 20 μg/ml). The PDGF-BB + inonotsuoxide B groups were treated with corresponding concentrations of inonotsuoxide B for 30 min at 37˚C. Thereafter, all groups except for the control were treated with 10 ng/ml PDGF-BB at 37˚C for 24 h. The MTT assay experimental procedure was performed as aforementioned. Cell viability or cytotoxicity calculation formula: Cell viability=[(mean absorbance sample-mean absorbance blank)/(mean absorbance control-mean absorbance blank)]*100.

Western blot analysis. HSC-T6 cells were seeded at a concentration of $1x10^5$/ml into a six-well culture plate and incubated at 37˚C with 5% CO_2. The cells were then divided

into the following five groups: Control, PDGF-BB (10 ng/ml) and PDGF-BB + inonotsuoxide B (5, 10 and 20 μg/ml). The processed cells were lysed in RIPA lysis buffer (Beyotime Institute of Biotechnology). Protein concentration was measured using the bicinchoninic acid protein assay kit (Beyotime Institute of Biotechnology) and the samples (50 μg) were subjected to 10% SDS-PAGE (11,12) and then transferred onto PVDF membranes, which were blocked with 5% skimmed milk at 25˚C for 3 h. Subsequently, rabbit anti-AKT, rabbit anti-p-ERK, rabbit anti-p-PI3K, rabbit anti-p-AKT, rabbit anti-ERK, rabbit anti-PI3K, rabbit anti-α-SMA, rabbit anti-COL-I and mouse anti-β-actin (all diluted 1:1,000) were added to the membranes and incubated at 4˚C overnight. The membranes were then incubated with horseradish peroxidase (HRP)-conjugated anti-rabbit or HRP-conjugated anti-mouse (all diluted 1:1,000) the following day for 1 h at room temperature, before the ECL chromogenic solution (Pierce; Thermo Fisher Scientific, Inc.) was added to develop the membrane (13). Finally, ImageJ software (version 1.8.0_101; National Institutes of Health) was used for the quantification of densitometry.

Reverse transcription-quantitative PCR (RT-qPCR). HSC-T6 cells were divided into the following five groups: Control, PDGF-BB (10 ng/ml) and PDGF-BB + inonotsuoxide B (5, 10 and 20 μg/ml). Cells in each group were collected and total RNA was extracted using TRIzol® reagent (Invitrogen; Thermo Fisher Scientific, Inc.). Briefly, 1 ml lysis buffer was added to the cells and incubated for 5 min at room temperature. Subsequently, 200 μl $CHCl_3$ was added, mixed with the cell extract via vigorous shaking and the solution was incubated for 10 min at room temperature. The samples were centrifuged (14,800 x g) at 4˚C for 30 min. The supernatant (400 μl) was collected and added to an equivalent volume of isopropyl alcohol. The mixture was stored at -20˚C for 2 h and centrifuged (14,800 x g) at 4˚C for 30 min. Subsequently, the supernatant was discarded and 1 ml of ethanol was added to each sample, which were centrifuged (14,800 x g) at 4˚C for 15 min. RNA was collected following air-drying for 10 min before 20 μl RNase-free water was added to dissolve the collected RNA, which was stored at -80˚C until subsequent analysis (14). According to the manufacturer's protocol, cDNA was synthesized by reverse transcription using Takara PrimeScript RT Master Mix kit (Takara Bio, Inc.). The temperature protocol was as follows: 15 min at 37˚C; 5 sec at 85˚C; and 10 min at 4˚C. qPCR was performed using SYBR®-Green Master Mix (Takara Bio, Inc.) according to the manufacturer's protocol. qPCR amplification was performed using β-actin as an internal reference. The following primer sequences were used: β-actin forward, 5'-CCGAGATCT CACCGACTACC-3' and reverse, 5'-TCCAGAGCGACA TAGCACAG-3' and α-SMA forward, 5'-TCCTCCTGAGCG CAAGTACTCT-3' and reverse, 5'-GCTCAGTAACAGTCC GCCTAGAA-3'. Pre-denaturation was performed at 95˚C for 30 sec, followed by 40 cycles of 95˚C for 5 sec and 60˚C for 30 sec (15). Quantification of the mRNA expression was performed using the $2^{-\Delta\Delta Cq}$ method (16,17).

Statistical analysis. Data are presented as the mean ± SEM. Statistical analysis was performed via one-way ANOVA followed by Tukey's post hoc test using GraphPad Prism v5 software (GraphPad Software, Inc.). Each group of experiments was performed ≥3 times. $P<0.05$ was considered to indicate a statistically significant difference.

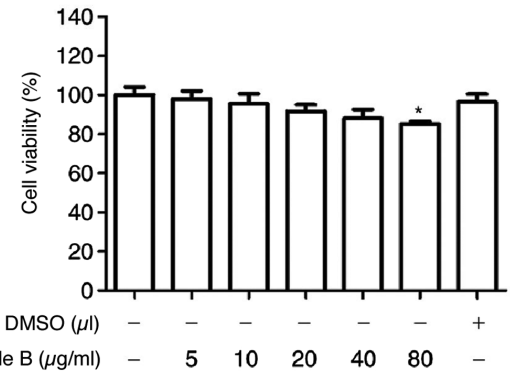

Figure 1. Effect of inonotsuoxide B on cell cytotoxicity in hepatic stellate cells. Hepatic stellate cells were treated with different concentrations of inonotsuoxide B for 24 h before cytotoxicity was measured using MTT assay. *P<0.05 vs. the control group (untreated cells).

Results

Effect of inonotsuoxide B on cell cytotoxicity. HSC-T6 cells were cultured with different concentrations of inonotsuoxide B dissolved in DMSO (5, 10, 20, 40 and 80 μg/ml) for 24 h. DMSO exhibited no effects on cell viability. Compared with that of the control group, inonotsuoxide B (5, 10, 20 and 40 μg/ml) exhibited only minor effects on cell viability (Fig. 1). However, cell viability was significantly reduced following incubation with 80 μg/ml of inonotsuoxide B. As a result, inonotsuoxide B at concentrations of 5, 10 and 20 μg/ml were used for subsequent experiments (Fig. 1).

Inonotsuoxide B reverses PDGF-BB-mediated increases in HSC viability. Compared with the control group, PDGF-BB (10 ng/ml) significantly increased the viability of HSC-T6 cells, which was in turn inhibited by inonotsuoxide B (5, 10 and 20 μg/ml) in a concentration-dependent manner (Fig. 2).

Inonotsuoxide B suppresses PDGF-BB-induced α-SMA mRNA expression in HSCs. The effect of inonotsuoxide B on the mRNA levels of α-SMA in HSCs was examined by RT-qPCR. As presented in Fig. 3, α-SMA mRNA expression in the PDGF-BB group was significantly increased compared with the control group. At concentrations of 5, 10 and 20 μg/ml, inonotsuoxide B significantly reduced the mRNA expression of α-SMA compared with the PDGF-BB group in a dose-dependent manner (Fig. 3).

Inonotsuoxide B suppresses the PDGF-BB-induced increases in α-SMA and COL-I protein expression in HSCs. The protein expression of the HSC activation markers α-SMA and COL-I was measured using western blotting. The protein expression levels of α-SMA and COL-I were significantly increased in the PDGF-BB group compared the control group, but were significantly decreased following inonotsuoxide B (10 and 20 μg/ml) treatment. By contrast, 5 μg/ml inonotsuoxide B did not exert

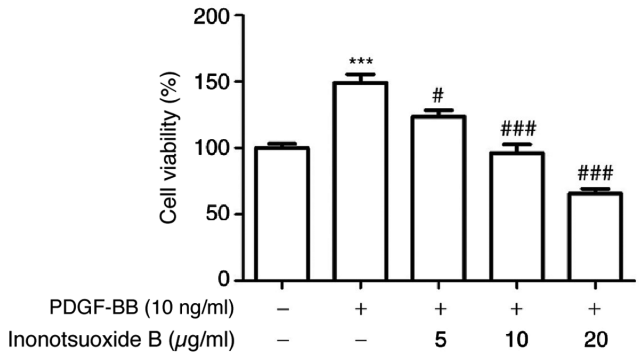

Figure 2. Effect of inonotsuoxide B on the PDGF-BB-induced potentiation of hepatic stellate cell viability. Cells were pretreated with different concentrations of inonotsuoxide B for 30 min before they were stimulated with PDGF-BB (10 ng/ml) for 24 h. ***P<0.001 vs. the control group (untreated cells); $^{\#}$P<0.05 and $^{\#\#\#}$P<0.001 vs. PDGF-BB. PDGF, platelet-derived growth factor.

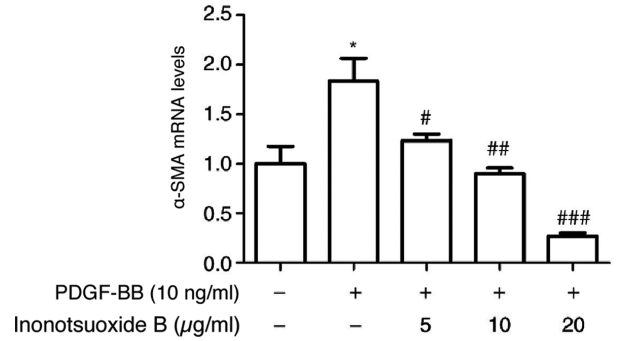

Figure 3. Effect of inonotsuoxide B on the PDGF-BB-induced increase of α-SMA mRNA expression in hepatic stellate cells. Cells were first treated with PDGF-BB (10 ng/ml) in serum-free DMEM for 24 h in the presence of inonotsuoxide B (5, 10 or 20 μg/ml). The expression of α-SMA was then determined using reverse transcription-quantitative PCR. *P<0.05 vs. the control group (untreated cells); $^{\#}$P<0.05, $^{\#\#}$P<0.01 and $^{\#\#\#}$P<0.001 vs. PDGF-BB. PDGF, platelet-derived growth factor; α-SMA, α-smooth muscle actin.

significant effects on the protein expression levels of α-SMA and COL-I compared with those in the PDGF-BB group (Fig. 4).

Inonotsuoxide B suppresses PDGF-BB-induced AKT, ERK1/2 and PI3K phosphorylation in HSCs. The phosphorylation of AKT, ERK1/2 and PI3K in each treatment group was measured via western blotting. As demonstrated in Fig. 5, the levels of AKT, ERK1/2 and PI3K phosphorylation were significantly increased in the PDGF-BB group compared with the control group. Treatment with inonotsuoxide B (5, 10 and 20 μg/ml) markedly reduced the levels of AKT and PI3K phosphorylation compared with those in the PDGF-BB group in a dose-dependent manner. However, the protein expression level of p-ERK was not significantly altered following treatment with 5 μg/ml innotsuoxide B, while p-ERK was significantly decreased after treatment with innotsuoxide B at 10 and 20 μg/ml.

PI3K inhibitor LY294002 suppresses PDGF-BB-induced α-SMA and COL-I expression in addition to AKT phosphorylation in HSCs. LY294002 is a specific blocker of the PI3K signaling pathway (18). The effects of LY294002 on the expression of the α-SMA, COL-I, AKT and ERK1/2 phosphorylation was examined by western blotting. As indicated in Fig. 6, the expression levels of α-SMA and COL-I proteins, in addition to AKT and ERK phosphorylation, were significantly increased in PDGF-BB-treated HSC-T6 cells compared with control cells. The expression levels of α-SMA, COL-I and AKT phosphorylation were also significantly decreased in the presence of LY294002, whilst LY294002 did not exert significant effects on ERK1/2 phosphorylation compared with the PDGF-BB group. Compared with the PDGF-BB group, the protein expression levels of α-SMA, COL-I, p-AKT and p-ERK1/2 in PDGF-BB + inonotsuoxide B (20 μg/ml) group were significantly reduced.

ERK inhibitor UO126 suppresses PDGF-BB-induced increases in α-SMA and COL-I expression in addition to ERK phosphorylation in HSCs. UO126 is a specific blocker of the ERK signaling pathway (19). The effect of UO126 on the expression of the α-SMA and COL-I in addition to AKT and ERK1/2 phosphorylation was examined via western blotting. As demonstrated in Fig. 7, the expression levels of α-SMA, COL-I, AKT phosphorylation and ERK phosphorylation were significantly increased in PDGF-BB-treated HSC-T6 cells compared with the control cells. The expression levels of α-SMA, COL-I and ERK phosphorylation were found to be significantly reduced in the UO126-treated group compared with those in the PDGF-BB group. By contrast, UO126 treatment did not result in significant effects on AKT phosphorylation compared with that in the PDGF-BB group. In addition, compared with the PDGF-BB group, the protein expression levels of α-SMA, COL-I, p-AKT and p-ERK1/2 in PDGF-BB + inonotsuoxide B (20 μg/ml) group were significantly reduced.

Discussion

The mechanism of liver fibrosis is complex (20). The proliferation and activation of HSCs and associated signaling pathways have been the focus of studies on liver fibrosis (21). However, research on potential treatments against liver fibrosis has primarily focused on singular targets and pathways. Consequently, treatments that are currently available for liver fibrosis have not always been effective (22). Previous studies have suggested that the chemical constituents of *Inonotus obliquus* (polysaccharide, inonot and betulin) exhibited anticancer, antiaging, blood sugar and blood pressure reducing pharmacological effects (23,24). Inonotsuoxide B is a tetracyclic triterpenoid that can be extracted from *Inonotus obliquus* and has been previously demonstrated to inhibit the growth of liver and gastric cancer cells (24). However, its effects on liver fibrosis remain poorly understood. The present study primarily focused on the effects of inonotsuoxide B treatment on HSC viability and activation with respect to the PI3K/AKT and ERK1/2 signaling pathways.

PDGF is an important mitogenic factor in HSC-T6 cells (2). During liver fibrosis, PDGF has been demonstrated to promote HSC proliferation and collagen expression (2). A previous study has reported that 10 ng/ml PDGF-BB stimulated the activation of HSCs (25). Therefore, the effect of inonotsuoxide B on HSC-T6 cells following treatment with PDGF-BB (10 ng/ml) was examined in the present study. Compared with those in the untreated cell group, PDGF-BB significantly increased the cell viability and activation of HSC-T6 cells, in addition to potentiating the expression of α-SMA and COL-I. Furthermore,

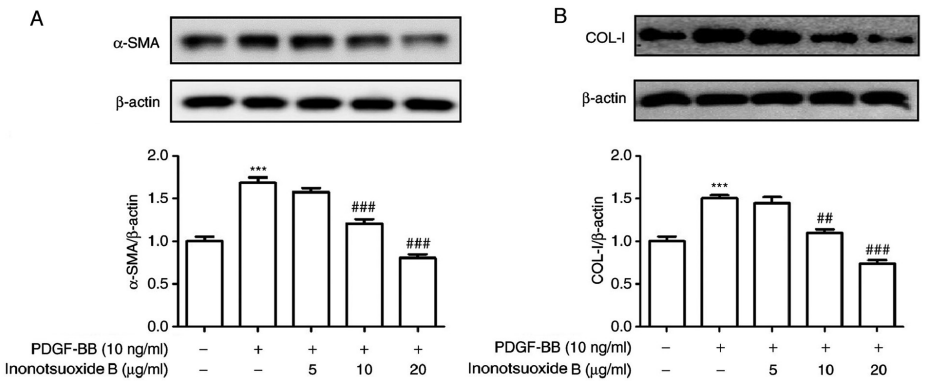

Figure 4. Effect of inonotsuoxide B on the PDGF-BB-induced increase of α-SMA and COL-I protein expression in hepatic stellate cells. Cells were treated with PDGF-BB (10 ng/ml) in serum-free DMEM for 24 h in the presence of inonotsuoxide B (5, 10 or 20 mg/ml). The expression levels of (A) α-SMA and (B) COL-I were measured by western blotting. ***P<0.001 vs. the control group (untreated cells); ##P<0.01 and ###P<0.001 vs. PDGF-BB. PDGF, platelet-derived growth factor; α-SMA, α-smooth muscle actin; COL-I, collagen I.

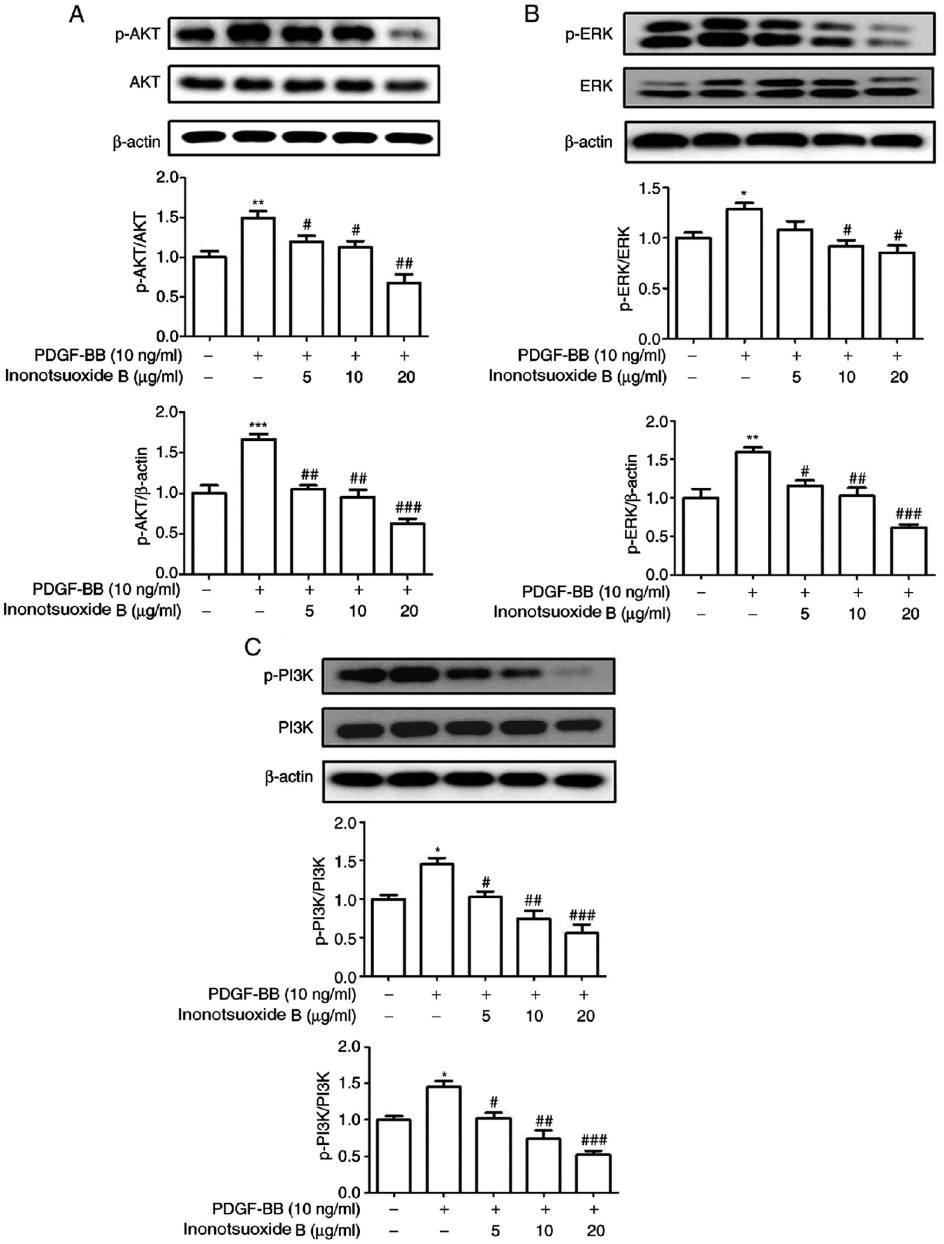

Figure 5. Effect of inonotsuoxide B on PDGF-BB-induced AKT, ERK1/2 and PI3K phosphorylation in hepatic stellate cells. The phosphorylation levels of (A) AKT, (B) ERK1/2 and (C) PI3K were measured by western blotting. *P<0.05, **P<0.01 and ***P<0.001 vs. the control group (untreated cells); #P<0.05, ##P<0.01 and ###P<0.001 vs. the PDGF-BB group. PDGF, platelet-derived growth factor; p, phosphorylated.

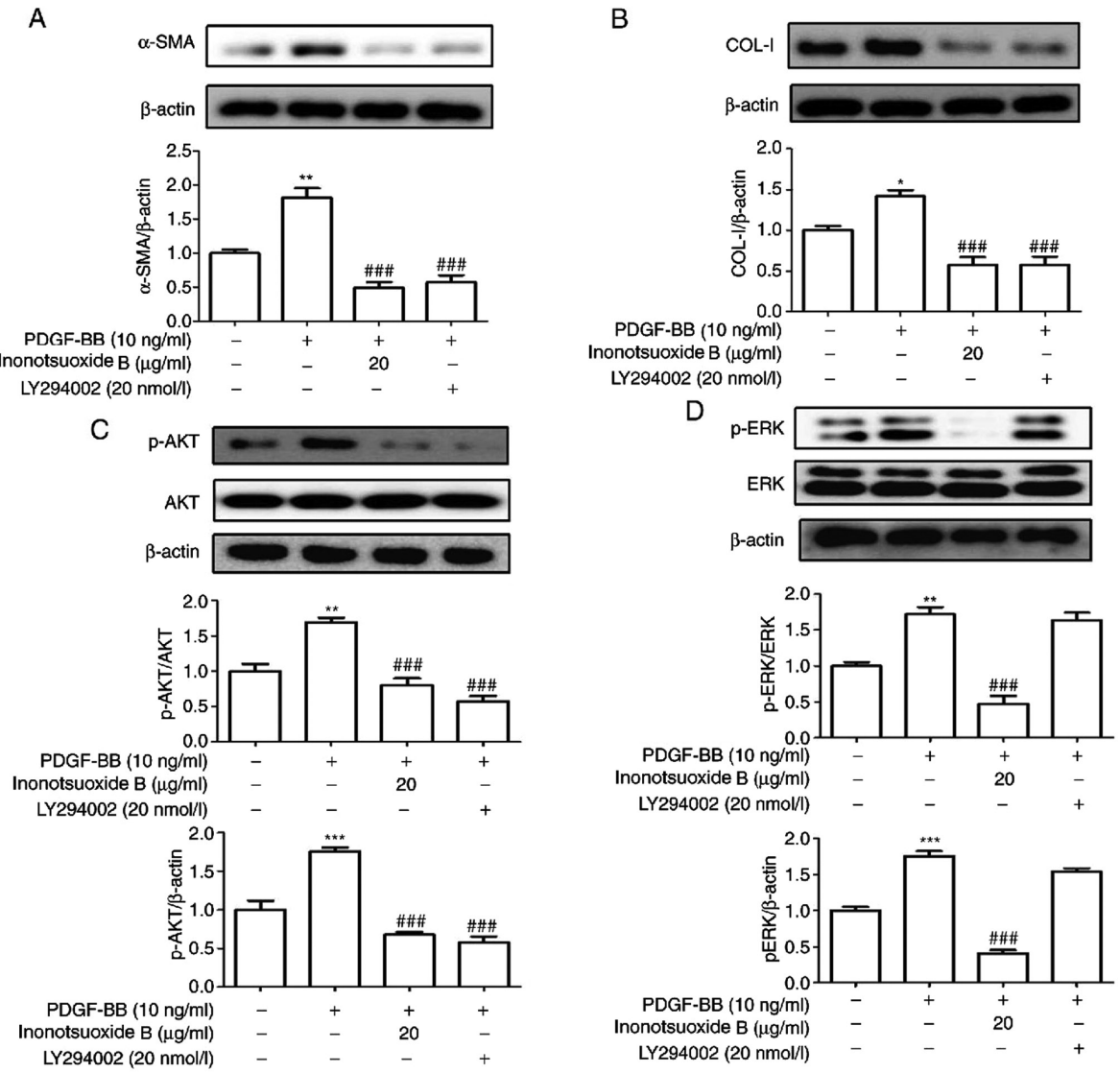

Figure 6. Effects of the PI3K inhibitor on PDGF-BB-induced increases of α-SMA and COL-I expression and AKT and ERK1/2 phosphorylation in hepatic stellate cells. The cells were treated with PDGF-BB (10 ng/ml) in the presence of LY294002 or with PDGF-BB (10 ng/ml) in the presence of inonotsuoxide B (20 μg/ml) in serum-free DMEM for 24 h. The expression levels of (A) α-SMA and (B) COL-I, and the phosphorylation levels of (C) AKT and (D) ERK1/2 were subsequently measured using western blotting. *P<0.05, **P<0.01 and ***P<0.001 vs. the control group (untreated cells); $^{###}$P<0.001 vs. the PDGF-BB group. PDGF, platelet-derived growth factor; α-SMA, α-smooth muscle actin; COL-I, collagen I; p, phosphorylated.

all of these aforementioned effects were reversed following treatment of the cells with inonotsuoxide B. These findings indicated that inonotsuoxide B reduced the viability and activation of PDGF-BB-stimulated HSC-T6 cells.

A previous study demonstrated that the PI3K/AKT and ERK signaling pathways primarily mediated PDGF-induced signaling (26). PI3K regulates the phosphorylation of AKT, where the subsequent PI3K/AKT downstream signaling pathway has been suggested to serve a regulatory role in a number of cell proliferation and activation processes (27). By contrast, the ERK signaling pathway has been reported to serve a key role in transducing signals from cell-surface receptors to the nucleus, thereby regulating the activation and proliferation of cells (28). Therefore, the phosphorylation of PI3K, AKT and ERK1/2 was examined in the present study. It was observed that the PI3K/AKT and ERK1/2 signaling pathways were associated with the inhibitory effects of inonotsuoxide B on the viability and activation of PDGF-BB-stimulated HSC-T6 cells. Compared with the untreated cell group, PDGF-BB treatment significantly upregulated the phosphorylation of PI3K, AKT and ERK in HSC-T6 cells, all of which were revealed to be reversed by inonotsuoxide B treatment. UO126 and LY294002 have been demonstrated to be specific blockers of the ERK and PI3K/AKT signaling pathways, respectively (29). Previous studies have reported that UO126 and LY294002 inhibited the proliferation of HSCs at concentrations <20 nmol/l, in a concentration-dependent manner (30,31). Therefore, in the present study, UO126 and LY294002 at 20 nmol/l were used to investigate their potential effects on PDGF-BB-induced HSC proliferation and activation. The results indicated that the expression levels of the α-SMA and COL-I proteins in PDGF-BB-stimulated HSCs were decreased by both UO126 and LY294002 treatments.

Liver fibrosis has been indicated to be reversible, as effective drug therapy can inhibit the activation and proliferation of HSCs and reduce the degree of hepatic fibrosis (32). The results of the present study demonstrated that inonotsuoxide B inhibited the

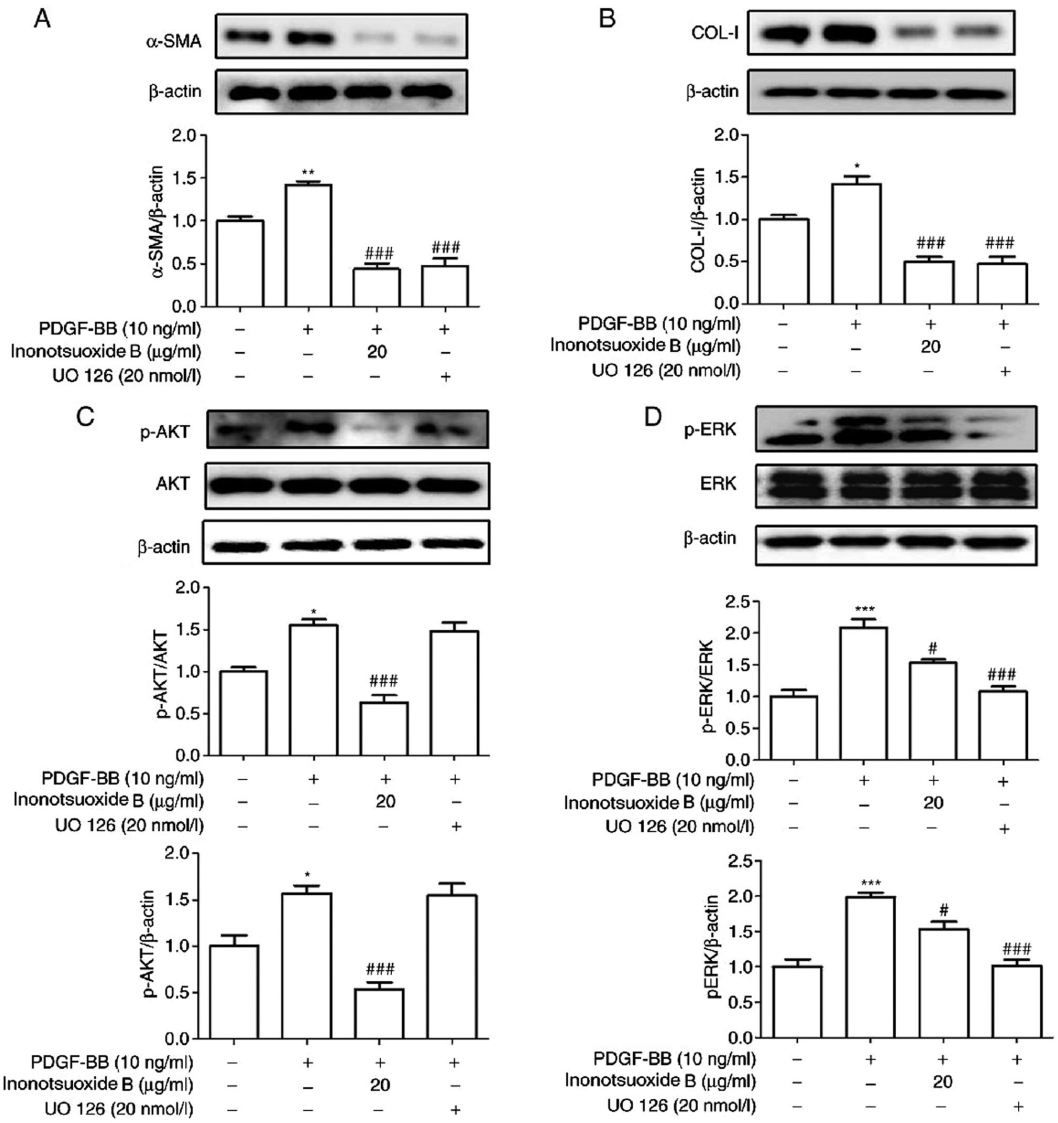

Figure 7. Effects of the ERK inhibitor on the PDGF-BB-induced increases of α-SMA and COL-I expression, in addition to AKT and ERK1/2 phosphorylation, in hepatic stellate cells. The cells were treated with PDGF-BB (10 ng/ml) in the presence of UO126 (20 nmol/l) or with PDGF-BB (10 ng/ml) in the presence of inonotsuoxide B (20 μg/ml) in serum-free DMEM for 24 h. The expression levels of (A) α-SMA and (B) COL-I, and the phosphorylation levels of (C) AKT and (D) ERK1/2, were measured using western blotting. *P<0.05, **P<0.01 and ***P<0.001 vs. the control group (untreated cells); $^{\#}$P<0.05 and $^{\#\#\#}$P<0.001 vs. the PDGF-BB group. PDGF, platelet-derived growth factor; α-SMA, α-smooth muscle actin; COL-I, collagen I; p, phosphorylated.

viability and activation of PDGF-BB-stimulated HSC-T6 cells. The underlying mechanism of action of inonotsuoxide B may be associated with the inhibition of the PI3K/AKT and ERK signaling pathways. These observations are clinically relevant and may enable the development of an efficient treatment strategy against liver fibrosis.

Acknowledgements

Not applicable.

Funding

The present study was funded by Research Fund for the Back-up Candidates of the Academic and Technical Leaders of Anhui, China (grant no. 2015H040), the Young top talents Program of Anhui Medical University, Foundation for Distinguished Young Talents in Higher Education of Anhui, China (grant no. gxyqZD2016049), the Natural Science Research Project in Higher Education of Anhui, China (grant no. KJ2017A192), the Hospital Youth Fund of West Branch of The First Affiliated Hospital of University of Science and Technology of China (grant no. 2018YJQN016), the Young Talent Support Plan of Anhui Medical University in 2017-2019 (grant no. 0601037104), 2018 Young Talents Double Training Project Grant (grant no. 0601037206), Science and Technology Fund of Anhui Province for Outstanding Youth of China (grant no. 1908085J30) and 2020-2022 Anhui Medical University Basic and Clinical Cooperative Research Promotion Project (grant no. 2019xkjT015).

Availability of data and materials

The datasets used and/or analyzed during the present study are available from the corresponding author on reasonable request.

Authors' contributions

YH and WC designed the current study. JJ and HY performed the experiments. LH and YW analyzed the data. CH drafted the manuscript and analyzed data. KW and ZW interpreted data and revised the final manuscript. WW performed the experiments and wrote the manuscript. JJ and YH confirm the authenticity of all the raw data All authors read and approved the final manuscript.

Ethics approval and consent to participate

Not applicable.

Patient consent for publication

Not applicable.

Competing interests

The authors declare that they have no competing interests.

References

1. Ping J, Li JT, Liao ZX, Shang L and Wang H: Indole-3-carbinol inhibits hepatic stellate cells proliferation by blocking NADPH oxidase/reactive oxygen species/p38 MAPK pathway. Eur J Pharmacol 650: 656-662, 2011.
2. Tsai MK, Lin YL and Huang YT: Differential inhibitory effects of salvianolic acids on activation of rat hepatic stellate cells by platelet-derived growth factor. Planta Med 77: 1495-1503, 2011.
3. Wang YH, Sun YC, Zuo LQ, Wang YN and Huang Y: ASIC1a promotes high glucose and PDGF-induced hepatic stellate cell activation by inducing autophagy through CaMKKβ/ERK signaling pathway. Toxicol Lett 300: 1-9, 2018.
4. Shuping You, Jun Zhao and Long Ma: Effects of total glycosides of cistanche deserticola on the proliferation of hepatic stellate cells induced by platelet-derived growth factor. Chin J Pharmacol 32: 1231-1235, 2016.
5. Choi JH, Hwang YP, Park BH, Choi CY, Chung YC and Jeong HG: Anthocyanins isolated from the purple-fleshed sweet potato attenuate the proliferation of hepatic stellate cells by blocking the PDGF receptor. Environ Toxicol Pharmacol 31: 212-219, 2011.
6. Youn MJ, Kim JK, Park SY, Kim Y, Kim SJ, Lee JS, Chai KY, Kim HJ, Cui MX, So HS, *et al*: Chaga mushroom (Inonotus obliquus) induces G0/G1 arrest and apoptosis in human hepatoma HepG2 cells. World J Gastroenterol 14: 511-517, 2008.
7. Duru KC, Kovaleva EG, Danilova IG and van der Bijl P: The pharmacological potential and possible molecular mechanisms of action of Inonotus obliquus from preclinical studies. Phytother Res 33: 1966-1980, 2019.
8. Kun WU, Wenming Cheng, Chunru Li, *et al*: Screening and chemical constituents of anti-tumor active parts of inonotus obliquus. J Anhui Medical University 51: 1468-1472, 2016.
9. Huang Y, Li X, Wang Y, Wang H, Huang C and Li J: Endoplasmic reticulum stress-induced hepatic stellate cell apoptosis through calcium-mediated JNK/P38 MAPK and Calpain/Caspase-12 pathways. Mol Cell Biochem 394: 1-12, 2014.
10. Foo NP, Lin SH, Lee YH, Wu MJ and Wang YJ: α-Lipoic acid inhibits liver fibrosis through the attenuation of ROS-triggered signaling in hepatic stellate cells activated by PDGF and TGF-β. Toxicology 282: 39-46, 2011.
11. Huang Y, Leng TD, Inoue K, Yang T, Liu M, Horgen FD, Fleig A, Li J and Xiong ZG: TRPM7 channels play a role in high glucose-induced endoplasmic reticulum stress and neuronal cell apoptosis. J Biol Chem 293: 14393-14406, 2018.
12. Wang H, Wang YH, Yang F, Li XF, Tian YY, Ni MM, Zuo LQ, Meng XM and Huang Y: Effect of Acid-sensing ion Channel 1a on the process of liver fibrosis under hyperglycemia. Biochem Biophys Res Commun 468: 758-765, 2015.
13. Li J, Li X, Xu W, Wang S, Hu Z, Zhang Q, Deng X, Wang J, Zhang J and Guo C: Antifibrotic effects of luteolin on hepatic stellate cells and liver fibrosis by targeting AKT/mTOR/p70S6K and TGFβ/Smad signalling pathways. Liver Int 35: 1222-1233, 2015.
14. Tsai TH, Shih SC, Ho TC, Ma HI, Liu MY, Chen SL and Tsao YP: Pigment epithelium-derived factor 34-mer peptide prevents liver fibrosis and hepatic stellate cell activation through down-regulation of the PDGF receptor. PLoS One 9: e95443, 2014.
15. Yujie Zhang, Yutao Hong and Lei Jie: Effects of melatonin on proliferation of HSC-T6 cells induced by PDGF-BB and its mechanism. J Anhui Med University 53: 12-17, 2018.
16. You SP, Zhao J, Ma L, Tudimat M, Zhang SL and Liu T: Preventive effects of phenylethanol glycosides from Cistanche tubulosa on bovine serum albumin-induced hepatic fibrosis in rats. Daru 23: 52, 2015.
17. Livak KJ and Schmittgen TD: Analysis of relative gene expres-sion data using real-time quantitative PCR and the 2(-Delta DeltaC(T)) method. Methods 25: 402-408, 2001.
18. Mazumder AG, Kumari S and Singh D: Anticonvulsant action of a selective phosphatidylinositol-3-kinase inhibitor LY294002 in pentylenetetrazole-mediated convulsions in zebrafish. Epilepsy Res 157: 106207, 2019.
19. Cole GW Jr, Alleva AM, Zuo JT, Sehgal SS, Yeow WS, Schrump DS and Nguyen DM: Suppression of pro-metastasis phenotypes expression in malignant pleural mesothelioma by the PI3K inhibitor LY294002 or the MEK inhibitor UO126. Anticancer Res 26: 809-821, 2006.
20. Lee UE and Friedman SL: Mechanisms of hepatic fibrogenesis. Best Pract Res Clin Gastroenterol 25: 195-206, 2011.
21. Bataller R and Brenner DA: Hepatic stellate cells as a target for the treatment of liver fibrosis. Semin Liver Dis 21: 437-452, 2001.
22. Wang Y, Gao J, Zhang D, Zhang J, Ma J and Jiang H: New insights into the antifibrotic effects of sorafenib on hepatic stellate cells and liver fibrosis. J Hepatol 53: 132-144, 2010.
23. Balandaykin ME and Zmitrovich IV: Review on chaga medicinal mushroom, inonotus obliquus (Higher Basidiomycetes): Realm of medicinal applications and approaches on estimating its resource potential. Int J Med Mushrooms 17: 95-104, 2015.
24. Glamočlija J, Ćirić A, Nikolić M, Fernandes Â, Barros L, Calhelha RC, Ferreira IC, Soković M and van Griensven LJ: Chemical characterization and biological activity of Chaga (*Inonotus obliquus*), a medicinal 'mushroom'. J Ethnopharmacol 162: 323-332, 2015.
25. Wang GJ, Huang YJ, Chen DH and Lin YL: *Ganoderma lucidum* extract attenuates the proliferation of hepatic stellate cells by blocking the PDGF receptor. Phytother Res 23: 833-839, 2009.
26. Jiang M, Wu YL, Li X, Zhang Y, Xia KL, Cui BW, Lian LH and Nan JX: Oligomeric proanthocyanidin derived from grape seeds inhibited NF-κB signaling in activated HSC: Involvement of JNK/ERK MAPK and PI3K/Akt pathways. Biomed Pharmacother 93: 674-680, 2017.
27. Kao YH, Chen PH, Wu TY, Lin YC, Tsai MS, Lee PH, Tai TS, Chang HR and Sun CK: Lipopolysaccharides induce Smad2 phosphorylation through PI3K/Akt and MAPK cascades in HSC-T6 hepatic stellate cells. Life Sci 184: 37-46, 2017.
28. Fang L, Zhan S, Huang C, Cheng X, Lv X, Si H and Li J: TRPM7 channel regulates PDGF-BB-induced proliferation of hepatic stellate cells via PI3K and ERK pathways. Toxicol Appl Pharmacol 27: 713-725, 2013.
29. He W, Shi F, Zhou ZW, Li B, Zhang K, Zhang X, Ouyang C, Zhou SF and Zhu X: A bioinformatic and mechanistic study elicits the antifibrotic effect of ursolic acid through the attenuation of oxidative stress with the involvement of ERK, PI3K/Akt, and p38 MAPK signaling pathways in human hepatic stellate cells and rat liver. Drug Des Devel Ther 9: 3989-4104, 2015.
30. Li Jinxing, Zhu Xianli and Li Yu: Rats with diffuse brain injury block the ERK pathway and down-regulate the expression of MMP-9 mRNA in brain tissue. Chin J Clin Neurosurg 11: 288-291, 2006.
31. You Linlin, Dai Lili, *et al*: Inhibitory effect of Danshensu on hepatic stellate cells stimulated by PDGF-BB. J Third Military Med University 33: 1610-1614, 2011.
32. Xu DD, Li XF, Li YH, Liu YH, Huang C, Meng XM and Li J: TIPE2 attenuates liver fibrosis by reversing the activated hepatic stellate cells. Biochem Biophys Res Commun 498: 199-206, 2018.